NIMBus: a Negative Binomial Regression based Integrative Method for Mutation Burden analysis

Jing Zhang 1/1/16 1:00 PM
Style Definition: Normal
Jing Zhang 1/1/16 12:58 PM
Style Definition: No Spacing

Jing Zhang[1,2], Jason Liu[2,3], Lucas Lochovsky[1], Jayanth Krishnan[1], Donghoon Lee[1], Mark Gerstein[1,2,4*]

[1]Program in Computational Biology and Bioinformatics, Yale University, New Haven, Connecticut 06520, USA
[2]Department of Molecular Biophysics and Biochemistry, Yale University, New Haven, Connecticut 06520, USA
[3]Program in Applied Math, Yale University, New Haven, Connecticut 06520, USA
[4]Department of Computer Science, Yale University, New Haven, Connecticut 06520, USA

* To whom correspondence should be addressed. Tel: +1 203 432 6105; Fax: +1 360 838 7861; Email: Mark.Gerstein@Yale.edu

ABSTRACT

Identification of somatic mutation hotspots as potential driver candidates in disease genomes is challenging because background mutation rate is usually heterogeneous and severely confounded by many known genomic features. Limited annotation information, especially in noncoding regions, further hinders the interpretability of the discovered candidates. Here, we address these issues with a new computational framework called NIMBus. It treats the varying mutation rates from different samples as a random variable with scaled gamma distribution and therefore models the over dispersed mutation count data by negative binomial distribution. To remove the confounding effect, we extracted 381 features from REMC and ENCODE in all available tissues and utilized a negative binomial regression to accurately estimate background mutation rate. Such integrative framework in NIMBus is flexible and can be immediately extended to accommodate any number of new features in the future. We also provided the most comprehensive noncoding annotation from ENCODE inside NIMBus to help users to better interpret the underlying biological mechanisms for the discovered targets. We applied NIMBus on 649 whole-genome cancer sequences and it successfully identified well-known noncoding drivers, such as the TERT promoter. We make LARVA available as a software tool, and release our results as an online resource (nimbus.gersteinlab.org).

1. Introduction

With the rapid development of high throughput sequencing technologies, thousands of whole genome sequencing (WGS) data for patients with various diseases considerably

increases the statistical power to dissect the mutation landscape at an unprecedented resolution. Frequently, scientists need to decide whether or not a region in a disease genome has more than the expected number of mutations, with somatic burden tests, to discover potential driver events that lead to complex diseases, such as cancer. Therefore, an accurate quantification of mutation burden is important to uncover the genetic cause of various diseases and then allow for targeted therapies in clinical studies. However, mutation burden test for somatic variants remains a challenge for several reasons.

First, many *state-of-the-art* methods are optimally designed for designed for analysis of coding regions, which usually represents less than 2 percent of the human genome. Nowadays, a myriad of studies have shown that noncoding mutations could serve as driver events for diseases. For example, the well-known noncoding mutations in TERT promoter were found to be associated with cancer progression in multiple cancer types. Hence, a unified coding and noncoding analysis is needed to annotate the discovered hotspots.

Second, some of the pioneer work analyzing WGS assumes a constant mutation rate across different regions or cancer genomes. However under this assumption, the mutation count data at the positional level often demonstrates larger than expected variances, resulting in many false positives and negatives. As a result, more sophisticated statistical models need to be introduced to handle such mutation heterogeneity in the somatic burden analysis.

Lastly, numerous functional characteristic features, such as replication timing, chromatin organization, and sequence context information, have been reported to largely affect somatic mutation process. Therefore, accurate mutational burden analysis should remove such covariate effect. Unfortunately, none of the few current methods that integrate limited covariates demonstrates acceptable model extensibility. For example, MutsigCV was one of the first methods to consider covariates in coding region burden tests by estimating local background mutation rate using a small neighborhood of genes with similar covariates. However, as the number of covariates increases, the '*curse of dimensionality*' will make it almost impossible to find a meaningful neighborhood in high dimension space. Similarly, Lochovsky *et al* only corrected replication timing with relatively low resolution. A large number of other genomic features were left behind in this methodology, and it is difficult to add them for further analysis under the same framework. Melton *et al* utilized a logistic regression framework to estimate a patient specific mutation rate at a single nucleotide resolution. Similar to MutsigCV, it only considered a limited number of covariates that explain a small part of variation in the mutation count data. Additionally in some quiet genomes with very few mutations such as Pilocytic Astrocytoma, usually there are less than 500 mutations across a single genome, resulting in poor model performance.

In this article, we propose a Negative Binomial Regression based Integrative Method for Mutation Burden analysis (NIMBus) that solves the three challenges mentioned above. It intuitively treats different somatic mutation rates from various disease genomes as random variables with a scaled gamma distribution, and resultantly models the mutation counts by a type I negative binomial distribution to handle overdispersion. In addition, to

capture the background mutational rate variation due to other genomic features, we integrate the most extensive features in all possible tissues from the Roadmap Epigenomics Mapping Consortium (REMC) to create a covariate table and use a negative binomial regression to predict the local mutation rate with high precision. We also summarized the most comprehensive noncoding annotations from the ENCODE project and used these biologically meaningful blocks as natural units to facilitate the understanding of our results. The integrative approach employed in NIMBus enables us to effectively pinpoint the mutation hotspots that are solely related with disease progression and better interpret their biological mechanisms.

2. Methods

2.1 WGS variants data used

We collected 649 whole genome variant calls from public resources and our collaborators. This data set contains a broad spectrum of 7 different cancer types (details in Text S1).

2.2 Covariate matrix generated from REMC and ENCODE data

First we divided the whole genome into bins with fixed length l. Then the bins that are overlapped with any of the two blacklist regions will be removed (details see Text S1). Then 381 features were extracted from both REMC and ENCODE, and average signal into these bins were calculated (details in Text S1). Let $x_{i,j}$ denote the average signal strength in the i^{th} bin and j^{th} covariate, where $i = 1, \cdots, n$ and $j = 1, \cdots, m$.

2.3 Noncoding annotations collection customized for NIMBus

We customized the full list of noncoding annotations from both ENCODE annotations and our previous efforts from our experience in 1000 genomes projects. This list include promoter regions, transcription start sites (TSS), translated regions (UTR), transcription factor binding sites (TFBS), enhancers, ultra-conserved, and ultra-sensitive sites. More details are given in Text S1.

2.4 Use negative binomial distribution to handle mutation count overdispersion caused by sample difference

Suppose there are $d = 1, \cdots, D$ different diseases (or disease types) in the collected WGS data, and $s = 1, \cdots, s_d$ represents samples for a specific type of disease d. Let $y_i^{d,s}$ and $\lambda_i^{d,s}$ denote the mutation counts and rate for the i^{th} bin in section 2.2 for sample s in disease d. In previous efforts, scientists assume that mutation rate $\lambda_i^{d,s}$ is constant across different regions of the human genome, samples, and diseases, so they have $\lambda_i^{d,s} \triangleq \lambda$ for

Jing Zhang 1/1/16 5:13 PM
Deleted: , including breast cancer (BRCA), gastric cancer (GACA), liver cancer (LICA), lung cancer (LUAD), prostate cancer (PRAD), Medulloblastoma (MB), and Pilocytic Astrocytoma (PA). Among these samples, 100 stomach cancer samples were from \cite{Wang}, and 95 prostate cancer samples were obtained from our collaborators. The remaining comes from samples published in Alexandrov

Jing Zhang 1/1/16 5:15 PM
Deleted: table

Jing Zhang 1/1/16 12:56 PM
Formatted: Normal

Jing Zhang 1/1/16 5:14 PM
Deleted: Numerous studies showed that several functional characteristics data will affect the local mutation rate, and such covariate effect should be removed during somatic burden analysis. In step one, we collected all the signal files from major histone modification marks, chromatin status, methylation, and mRNA-seq data from the REMC at a 20 nucleotides resolution. W ... [1]

Jing Zhang 1/1/16 12:56 PM
Deleted: lists from ENCODE projects

Jing Zhang 1/1/16 5:15 PM
Deleted: collected

Jing Zhang 1/1/16 5:16 PM
Deleted: ,

Jing Zhang 1/1/16 5:16 PM
Deleted: which include

Jing Zhang 1/1/16 5:17 PM
Deleted: Promoters and TSS sites were defined as the 2500 and 100 nucleotides ... [2]

Jing Zhang 1/1/16 2:58 PM
Deleted: Negative binomial based burden analysis model

Jing Zhang 1/1/16 3:47 PM
Formatted: Not Raised by / Lowered by

Jing Zhang 1/1/16 3:47 PM
Formatted: Not Raised by / Lowered by

Jing Zhang 1/1/16 3:48 PM
Formatted: Not Raised by / Lowered by

Jing Zhang 1/1/16 3:53 PM
Formatted: Not Raised by / Lowered by

Jing Zhang 1/1/16 3:55 PM
Formatted: Not Raised by / Lowered by

$\forall\, i, d, s$. Hence $y_i^{d,s}$ follows a Poisson distribution with the probability mass function (PMF) given in equation (1).

$$p_{Y_i^{d,s}}\left(y_i^{d,s}\right) = \frac{e^{-\lambda_i^{d,s}}\left(\lambda_i^{d,s}\right)^{y_i^{d,s}}}{y_i^{d,s}!} \triangleq \frac{e^{-\lambda}\lambda^{y_i^{d,s}}}{y_i^{d,s}!} \quad (1)$$

However, somatic genomes are highly heterogeneous because regions from different disease, samples, and sections of the same genome usually demonstrate very different mutation rates, severely violating assumptions in equation (1). This violation usually result in a larger than expected variance in $y_i^{d,s}$, and this phenomenon is called mutation count overdispersion. It will generate numerous false positives and needs to be carefully calibrated in somatic burden analysis. In our model, we first pool all the samples from the same disease d together and count the mutations in region i as

$$y_i^d = \sum_{s=1}^{S_d} y_i^{d,s} \quad (2)$$

Then we try to model y_i^d to better handle overdispersion. Assume that $\lambda_i^d = \sum_s \lambda_i^{d,s}$ represent the overall mutation rate from all samples in region i of disease type d. Different from the constant mutation rate assumption in (1), we instead assume that λ_i^d is a random variable with a scaled gamma distribution (Γ) with parameter μ_i^d and σ_i^d in equation (3).

ACROSS s

$$\lambda_i^d = \mu_i^d \gamma_i^d, \quad \gamma_i^d \sim \Gamma\left(1, \frac{1}{\sigma_i^d}\right) \quad (3)$$

Then the conditional distribution of y_i^d given λ_i^d can be represented as a Poisson distribution with PMF in (4).

$$p_{Y_i^d}\left(y_i^d \middle| \lambda_i^d\right) = \frac{e^{-\lambda_i^d}\lambda^{y_i^d}}{y_i^d!} \quad (4)$$

By integrating (3) into (4), the marginal distribution of y_i^d can be represented by a type I negative binomial distribution with PMF in (5).

$$p_{Y_i^d}\left(y_i^d \middle| \mu_i^d, \sigma_i^d\right) = \frac{\Gamma\left(y_i^d + 1/\sigma_i^d\right)}{\Gamma\left(1/\sigma_i^d\right)\Gamma\left(y_i^d + 1\right)}\left(\frac{\sigma_i^d \mu_i^d}{1+\sigma_i^d \mu_i^d}\right)^{y_i^d}\left(\frac{1}{1+\sigma_i^d \mu_i^d}\right)^{1/\sigma_i^d} \quad (5)$$

The mean and variance of y_i^d can be described as μ_i^d and $\mu_i^d\left(1+\sigma_i^d\right)$ respectively. Our model in equation (5) is convenient with explicit interpretability. First it automatically incorporates the sample mutation rate differences. For region i of disease

Jing Zhang 1/1/16 3:55 PM
Formatted: Not Raised by / Lowered by

Unknown
Field Code Changed

Jing Zhang 1/1/16 1:40 PM
Formatted: No Spacing

Jing Zhang 1/1/16 2:45 PM
Formatted: No Spacing, Right

Unknown
Field Code Changed

Jing Zhang 1/1/16 2:45 PM
Formatted: Not Raised by / Lowered by

Jing Zhang 1/1/16 2:45 PM
Formatted: Not Raised by / Lowered by

Jing Zhang 1/1/16 1:40 PM
Formatted: No Spacing

Jing Zhang 1/1/16 3:58 PM
Formatted: Not Raised by / Lowered by

Jing Zhang 1/1/16 4:00 PM
Formatted: Not Raised by / Lowered by

Unknown
Field Code Changed

Jing Zhang 1/1/16 2:53 PM
Formatted: No Spacing, Right

Unknown
Field Code Changed

Unknown
Field Code Changed

Unknown
Field Code Changed

Jing Zhang 1/1/16 3:08 PM
Formatted: Not Raised by / Lowered by

Jing Zhang 1/1/16 1:53 PM
Formatted: No Spacing

Jing Zhang 1/1/16 3:08 PM
Formatted: Not Raised by / Lowered by

Jing Zhang 1/1/16 3:08 PM
Formatted: Not Raised by / Lowered by

d, the individual contribution of mutation rate $\lambda_i^{d,s}$ from each sample s may vary as a random variable, and resultantly the overall mutation rate λ_i^d in (3) is not a constant anymore. Second, our model in (5) clearly separates the two main parameters μ_i^d and σ_i^d with physically interpretable meaning: the mean and over-dispersion. Here a larger σ_i^d indicates a more severe degree of overdispersion, which is usually due to larger difference in $\lambda_i^{d,s}$ across different samples.

2.5 Effective local background rate estimation by effective covariate correction through negative binomial regression

After modeling y_i^d using negative binomial distribution in 2.4, we then tried to estimate the local mutation rate by correcting the covariate table $\boldsymbol{X}$ described in 2.2. Again $x_{i,j}$ denote the average signal strength in the i^{th} bin and j^{th} covariate, where $i = 1, \cdots, n$ and $j = 1, \cdots, m$. Because we noticed that the genomic features in the covariate tables are highly correlated, which may introduce multicollinearity if directly used in the regression model, we first applied principle component analysis (PCA) to matrix $\boldsymbol{X}$. Let $\boldsymbol{X}'$ represent the covariate matrix after PCA and $x'_{i,j}$ denote each element in matrix $\boldsymbol{X}'$.

A generalized regression scheme is used here. Suppose g_1 and g_2 are two link functions. We then use linear combinations of covariate matrix $\boldsymbol{X}'$ to predict the transformed mean parameter μ_i^d and overdispersion parameter σ_i^d as

$$g_1\left(\mu_i^d\right) = \log\left(\mu_i^d\right) = \beta_0 + \beta_1 x'^d_{i,1} + \cdots + \beta_j x'^d_{i,j} + \cdots + \beta_m x'^d_{i,m}$$
$$g_2\left(\sigma_i^d\right) = \log\left(\sigma_i^d\right) = \alpha_0 + \alpha_1 x'^d_{i,1} + \cdots + \alpha_j x'^d_{i,j} + \cdots + \alpha_m x'^d_{i,m} \quad (6).$$

Here we used the log function for g_1 and g_2 since y_i^d follows a negative binomial distribution, then the regression model in (6) is also called a negative binomial regression. We used the GAMLSS package in R to estimate the parameters in (6) as $\hat{\alpha}_0^d, \cdots, \hat{\alpha}_m^d, \hat{\beta}_0^d, \cdots, \hat{\beta}_m^d$.

For the k^{th} target region, we first extend this target region into length l selected in section 2.2. Then within this extended bin, we calculate the average signal for feature j as $x_{k,j}^d, j = 1, \cdots m$, and after PCA projection, $x'^d_{k,j}$ represents the value for the j^{th} PC. Then the local mutation parameters $\hat{\mu}_k^d$ and δ_k^d in the extended bin for the k^{th} target region can be calculated as

$$\hat{\mu}_k^d = \exp\left(\hat{\beta}_0 + \hat{\beta}_1 x'^d_{k,1} + \cdots + \hat{\beta}_j x'^d_{k,j} + \cdots + \hat{\beta}_m x'^d_{k,m}\right)$$
$$\hat{\sigma}_k^d = \exp\left(\hat{\alpha}_0 + \hat{\alpha}_1 x'^d_{k,1} + \cdots + \hat{\alpha}_j x'^d_{k,j} + \cdots + \hat{\alpha}_m x'^d_{k,m}\right) \quad (7).$$

In reality, l_k, length of the k^{th} test region that could be an enhancer or promoter for example, is much shorter than the length of our training bins (l in section 2.2, might be up to 1Mb). Hence $\hat{\mu}_k^d$ need to be adjusted by a factor of l_k/l for the length effect. Then

Jing Zhang 1/1/16 5:52 PM
Comment [1]: This part is not clear. Do you suggest we mention the same sigma assumption in the supplementary? I am afraid that reviewers will ask

Jing Zhang 1/1/16 5:51 PM
Formatted: Highlight

Jing Zhang 1/1/16 5:51 PM
Formatted: Highlight

Jing Zhang 1/1/16 3:08 PM
Formatted: Not Raised by / Lowered by

Jing Zhang 1/1/16 4:33 PM
Formatted: Font:Not Bold

Jing Zhang 1/1/16 4:50 PM
Formatted: No Spacing

Unknown
Field Code Changed

Jing Zhang 1/1/16 4:11 PM
Formatted: Not Raised by / Lowered by

Jing Zhang 1/1/16 4:11 PM
Formatted: Not Raised by / Lowered by

Jing Zhang 1/1/16 4:11 PM
Formatted: No Spacing, Right

Jing Zhang 1/1/16 4:38 PM
Formatted: No Spacing

Jing Zhang 1/1/16 4:28 PM
Formatted: No Spacing, Right

Unknown
Field Code Changed

Jing Zhang 1/1/16 4:28 PM
Formatted: Not Raised by / Lowered by

Jing Zhang 1/1/16 4:28 PM
Formatted: Not Raised by / Lowered by

Jing Zhang 1/1/16 4:50 PM
Formatted: No Spacing

δ_k^d and the adjusted $\hat{\mu}_k^d$ can be used to calculate to p_k^d to indicate how likely this test region is with more than expected mutations through negative binomial distribution. This scheme is usually computationally expensive because in a typical test there are millions of functional elements to be tested, and to calculate the average signal for all features in the extended target bin takes a long time. Therefore, we proposed a gridding method to approximate the optimal $\hat{\mu}_k^d$ and δ_k^d in our analysis (details see Text S1).

2.6 Combining P values for multiple disease types

Sometimes several related diseases, or diseases of different subtypes needs to be analyzed together to provide a combined P value. One typical example is the pan-cancer analysis. In section 2.5, we calculated the P value for disease/disease type d as p_k^d in test region k. Specifically, the test statistic can be calculated in (8)

$$T_k = -2\sum_{d=1}^{D} \ln\left(p_k^d\right) \sim \chi^2(2D) \quad (8).$$

Here T_k follows a centered chi-square distribution with degree of freedom $2D$, where D is total number of diseases/disease types. Then the final P value for p_k can be calculated accordingly.

2.7 Training bin size selection

There are pros and cons to select certain a bin size for model training. On one hand, a shorter bin size will be advantageous in the P value evaluation as it can more effectively remove the heterogeneity in the local mutation process at a higher resolution. On the other hand, it sometimes will result in worse regression performance when estimating μ and δ. One reason is that in order to effectively estimate the mutation rate change with covariates, we need to obtain sensible mutation rate estimation in each single bin. However on the 3 billion bases genome, somatic mutation count data is usually sparse due to limited number of disease genomes available at the moment. In the extreme case, when the bin size is small enough so that most bins have mutations, it is difficult for the regression model to capture the relationship between mutations and covariates. Another reason is that some of the covariates are only reported to be functional in a large scale, so reducing the bin size will not necessarily introduce better prediction precision. The best bin size selection for the training purpose is still a challenging question that needs further case-by-case investigation. In our analysis, we used a 1mb bin size for all cancer types.

2.8 Flowchart of NIMBus

To better illustrate how NIMBus works, its workflow is given in Figure 1.

Jing Zhang 1/1/16 5:02 PM
Moved (insertion) [1]

Jing Zhang 1/1/16 5:08 PM
Formatted: No Spacing, Right

Unknown
Field Code Changed

Jing Zhang 1/1/16 5:10 PM
Formatted: No Spacing

Jing Zhang 1/1/16 5:12 PM
Deleted: Since regression is run separately on each single disease/subtype of disease, either Fisher's method can be used to combine the P values together. ... [3]

Jing Zhang 1/1/16 5:02 PM
Deleted: 5

Jing Zhang 1/1/16 5:02 PM
Moved up [1]: 2.6 Combining P values

Jing Zhang 1/1/16 5:12 PM
Deleted: 2.6 Combining P values ... [4]

Jing Zhang 1/1/16 5:02 PM
Deleted: 7

3. Results

3.1. Heterogeneity from various sources leads to large overdispersion in mutation counts data

Figure 1. Flowchart of NIMBus

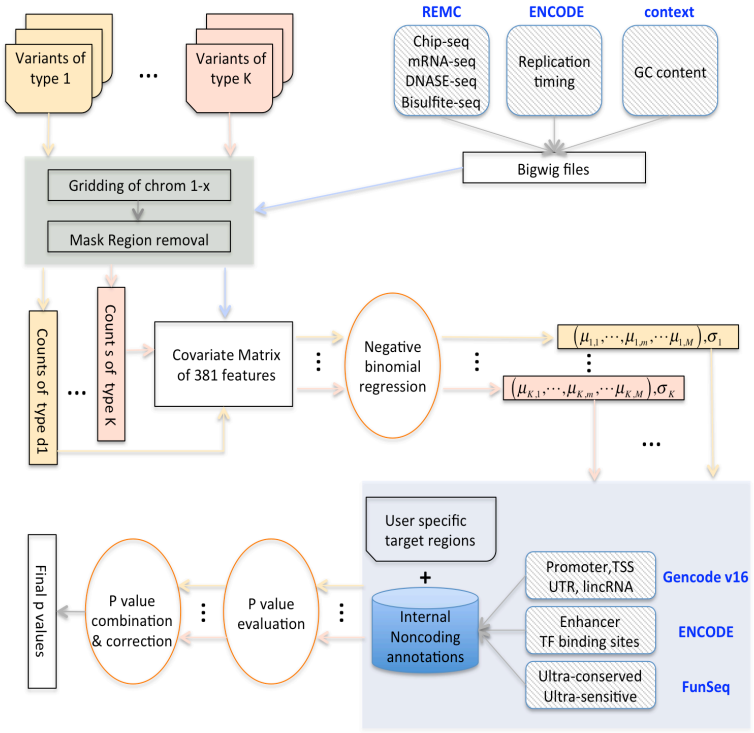

Pioneer genome wide somatic burden analysis usually assumes a homogeneous mutation rate, which consequently uses binomial or Poisson tests to evaluate P values. However, we found that mutation count data usually violates such an assumption because there are various sources of heterogeneity in the mutation rate. To demonstrate this, we collected WGS variants from 649 cancer patients and 7 cancer types as shown in Fig. 2A. First, we found that mutation count per genome varies from disease to disease. For instance, the median number of variants can be as low as 70 in PA and as high as 21287 in LUAD

Figure 2. Mutation rate heterogeneity from various sources result in huge overdispersion in mutation count data. (A) Sample numbers for each cancer type in our analysis; (B) boxplots and scatter plots of mutation counts per sample; (C) summary of mutation counts; (D) fitting of Poisson and Negative binomial distribution

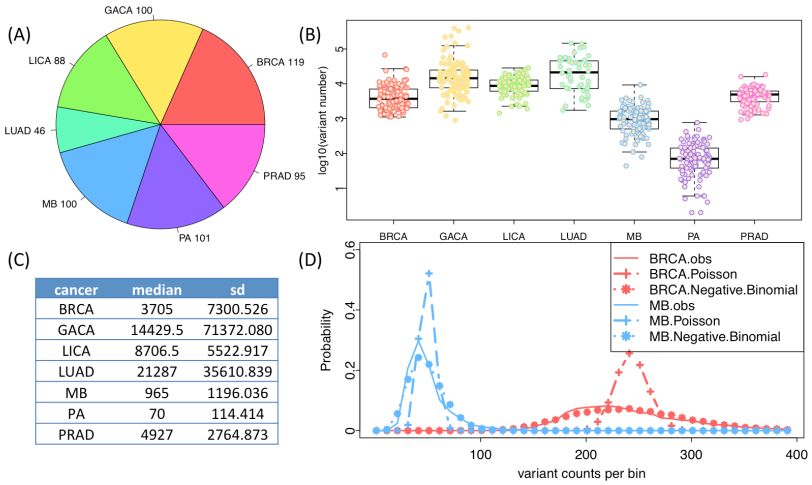

cancer	median	sd
BRCA	3705	7300.526
GACA	14429.5	71372.080
LICA	8706.5	5522.917
LUAD	21287	35610.839
MB	965	1196.036
PA	70	114.414
PRAD	4927	2764.873

(Fig. 2B-C). Even within the same disease, mutation rate may dramatically change from sample to sample (lowest at1743 and highest at 145500 in LUAD). In addition, there are also large regional mutation rate differences within the same sample (Fig. 3). Therefore, a binomial or Poisson distribution usually provides poor fitting to the real mutation counts data (Fig. 2D, dash lines with +). In light of these, we utilized a two parameter negative binomial distribution to further capture the overdispersed nature of mutation counts data, which improves fitting to real data significantly (dash lines with star in Fig. 2D).

3.2 Local mutation rate is confounded by other genomic features

Instead of homogeneously located across the genome in a random way, somatic mutation rate has been reported in literature to be confounded by several genomic features. For example, single stranded DNA during replication usually suffers from endogenous DNA damage, such as oxidation and deamination. Therefore, the accumulative damage effect in the later replicated regions will result in elevated mutation rate. Another well-known factor is the expression levels. The highly expressed regions often demonstrate lower mutation rate as compared to lowly expressed regions due to the transcription-coupled repair mechanism \{cite Mutsig and refer}. Furthermore, it has been reported that the chromatin organization, which arranges the genome into heterochromatin- and euchromatin-like domains, has a dominant influence on regional mutation-rate variation in human somatic cells \{cite 22820252}. We also find a similar trend in our data analysis. For instance, the normalized mutation rate of the first 100 1mb bins extracted in 95 breast cancer samples was plotted in the black line in Fig. 3. It is notably correlated with GC content (red line) and chromatin accessibility (blue line) in matched breast tissue.

Figure 3. Local mutation rate is correlated with many genomic features. The black line is the normalized mutation rate in 95 breast cancer sample. Normalized GC content (red line) and Chromatin accessibility (blue line) were significantly correlated with mutation rate.

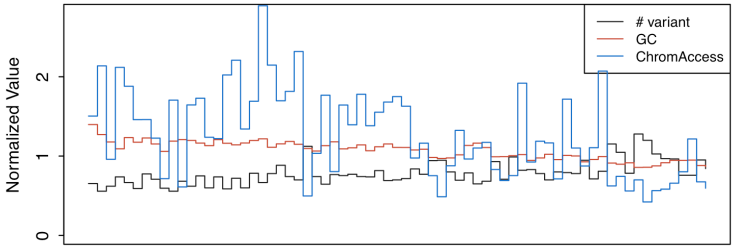

3.3. Negative binomial regression precisely estimates local mutation rates by correcting a list of genomic features

In light of the high correlation of individual genomic features with mutation rate in all cancer types, we try to investigate the joint collaborative effect of multiple features to predict mutation rate. It has been reported that most accurate prediction can be achieved by using the matched tissue. Hence, we specifically selected variants in two distinct cancer types BRCA and MB and predict their local mutation rate by features from different tissues. Relative error of each 1mb bin is defined by the absolute value of observed and predicted difference divided by the observed value and its mean value over all bins is used to compare the regression performance. As expected, regression using matched tissue features provides the lowest relative error. For example, using MB related features to predict variant counts in MB has a mean relative error of 0.183, less than that using BRCA features for MB (Fig. 4B, P value of two sided Wilcoxon test $< 2.2e^{-16}$).

However, non-matched tissue regression still provides insightful information during regression. For example, even when MB features are used to predict BRCA mutation rates, a decent although slightly poorer performance can still be achieved (0.135 for unmatched vs. 0.128 for matched). One explanation is that these genomic features are highly correlated both within and across different tissues. A correlation plot is given in Fig. 4A. Size and darkness of color of each dot inside the matrix represent the absolute value of Pearson correlation, while blue and red represents positive and negative values respectively. Usually histone modification marks within the same tissue provides the highest correlation (e.g H3k4me1, H3k4me3, H36k4me3). However, these features in MB are also significantly associated with those in BRCA. That is why these signals can be imputed using interpolation through data in other tissues \{cite 25690853}. This conclusion is important for two reasons: (1) tissue matching is usually extremely difficult for complex disease such as cancer. For example, there are several sets of covariates for breast tissues in REMC, which come from different parts of breast tissue. However, the exact tumor location data is sometimes vaguely described or even missing. (2) Even if the perfectly matched tissue can be identified in some cases, the data matrix from REMC is far from complete. In our example, methylation data for breast tissue of this particular

Figure 4. (A) Genomic features are highly correlated. B_* represents breast cancer related features and M_* indicates Medulloblastoma related features. (B) relative error of average mutation rate in each 1mb bin by different regressions. (C) Regression performance against number of PCs used in the regression. (D) performance of regression for all cancer types.

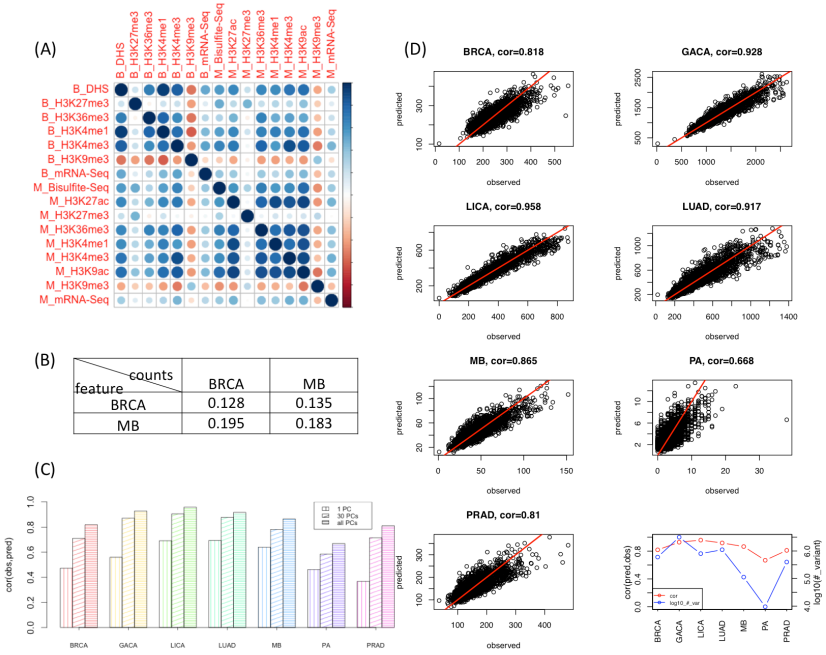

type is missing (Fig. 4A). Another example is that there is no prostate tissue in REMC, so there is no matched for prostate cancer. We still need to predict the local mutation rate in prostate cancer so correlated features in other related tissues would still provide additional information to boost regression performance.

To overcome the multi-collinearly problem due to the correlated nature of genomic features, we first performed a principle component analysis (PCA) on the 381 features. The first principle component (PC) could explain up to 55.69% of variance in the covariate matrix. It takes at least 15 and 106 PCs to capture 90% and 99% of variance respectively. However, PCA based regression is very sensitive to the PCs selected because sometimes the PCs that can best explain the variance in the mutation count data is not necessarily those that can best explain the variance in the covariate matrix. Hence, for each cancer type, we first ranked the individual PCs, and then only select the top 1, 30, and all PCs to predict the local mutation rate. Fig. 4C shows that in all 7 cancer types, using more PCs can noticeably boost prediction performance. For example, in BRCA the Pearson correlation is only 0.472 if 1 PC is used in regression. However, correlation coefficient can rise to 0.655 and 0.709 if 15 and 30 PCs are used respectively, and it can eventually be increased to 0.818 after using all PCs. As a result, in all the following analysis, we used all PCs for accurate local mutation rate estimation.

Our PCA based negative binomial regression can precisely capture the effect of various genomic features on somatic mutation process and accurately predict the local mutation rate in all cancer types. The Pearson correlations of the observed data and the predicted value vary from 0.668 in PA to 0.958 in LICA. Scatter plots are given in Fig. 4D. It is worth mentioning that although there is no prostate tissue in REMC data, we can still achieve a very decent correlation of 0.81 with the help of 381 unmatched but correlated features. It indicates that when somatic mutation data of an unknown disease is given, our model could still achieve acceptable performance without the knowledge of related tissue information. In addition, our regression performance is affected but not limited to the total number of variants (bottom right figure in Fig. 4D). Obviously limited number of mutations could restrict the prediction precision, such as in very quiet somatic genomes like PA (lowest correlation at 0.668 among 7 cancer types). Other factors, such as number of effective covariates, quality of mutation calls, and molecular similarity of pooled samples of the same disease could also considerably influence the performance of our model. For instance, although there are a smaller number of variants in MB than in BRCA, our regression in MB still outperforms that in BRCA (0.865 VS. 0.818, Fig. 4D).

3.4. NIMBus discovered a list of highly recurrent noncoding regions from cancer WGS data

We applied NIMBus on WGS variant calls on all 7 cancer types to deduce the individual somatic burden P values, and compared with the results from global and local Poisson models (details in section 2.4). As expected, both global and local Poisson models generated obviously too many burdened regions in all noncoding annotation categories because of the poor fitting of Poisson distributions to the mutation count data (Fig. 2D). For example, in the promoter regions, after P value correction, NIMBus provided 8 promoters as highly mutated, while local and global Poisson models identified 47 and

406 respectively. It is very unlikely that in a single tissue, all these 47 or 406 promoters are all linked with tumor progression. Hence, our negative binomial assumption in NIMBus effectively captured the overdispersion and controlled the number of false positives. To further demonstrate this, we provided the Q-Q plots of P values from all 7 cancer types were provided in Fig. 5B as quality check. In theory, if no significantly burdened regions are detected, the P values should follow uniform distribution. As it is seen in Fig. 5B, in all cancer types the majority of our P values for all cancer types follows the uniform assumption with a few outliers as the true signals, indicating reasonable P value distributions. Similar results have also been seen in other noncoding annotations (data not shown).

To summary the mutation burdens from all cancer types, we used Fisher's method to calculate the final P values for all three models. Similar to P values from a single cancer type, the combined P values are severely inflated in both global and local Poisson models, but are rigorously controlled by NIMBus (table C in Fig. 5). Take the TSS as an example, NIMBus reported only 65 sites as burdened, as compared with 273 and 465 for the other two methods. Additional, out of the 65 TSS elements, several of them have been experimentally validated or computationally predicted as associated with cancer in other work. For instance, TP53 is a well-studied oncogene that is related in many cancer types, and combined P value for TP53 TSS is ranked second in our analysis (P=4.26e−14). LMO3 interacts with the tumor suppressor TP53 and regulates its function, and it is ranked fourth in our analysis (P=3.25e−13). We also found that the fifth ranked gene RMRP (p=1.36e−10), which is the RNA component of mitochondrial RNA processing endoribonuclease, has been claimed to be associated with colorectal and breast cancers \{cite 26415221}. Another important example is the TSS sites in TERT, which is ranked sixth in our results (p=1.55e−10) and has been experimentally validated as associated with multiple types of cancer progression. The discovery of such validated results proved that NIMBus can serve as an powerful tool for driver events discovery in diseases.

4. Discussion

Fig. 5 (A) number of detected prompter regions in all cancer types; (B) Q-Q plots of P values for promoter regions; (c) total number of over burdened regions in our noncoding annotations after merging P values from 7 cancer types. P_local: local Poisson Model, P_global: global Poisson Model

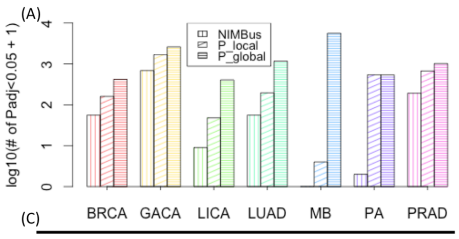

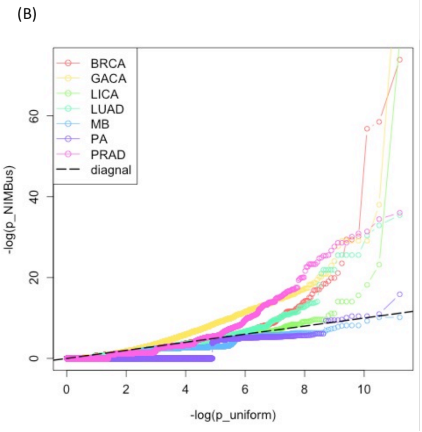

(C)

Annotation	N	NIMBus	P_local	P_global
DRM	13896	6	93	125
promoter	72840	113	1151	2442
UTR	154885	39	220	487
TSS	195586	65	273	465
Uconserved	481	1	1	1
Usensitive	1352	30	109	61
DHS	2887731	592	3908	6332
TFBS	5712328	2854	22721	46357

Thousands of somatic genomes are now available due to the fast development of whole genome sequencing technologies, providing us with increasing statistical power to scrutinize the somatic mutation landscape. At the same time, thanks to the collaborative effort of big consortiums, such as REMC and ENCODE, tens of thousands of functional characteristic data on human genomes has been released for immediate use to the whole community. Hence, integrative frameworks are of urgent need to explore the interplay between WGS data and the functional characteristic data. It will not only be important to accurately search for mutational hotspots as driver candidates for complex diseases but also to better interpret the underlying biological mechanism for clinicians and biologists.

In this paper, we proposed a new integrative framework called NIMBus that uses a negative binomial regression to capture the effect of a widespread list of genomic features on mutation processes for accurate somatic burden analysis. Due to the heterogeneous nature of various somatic genomes, our model treated the mutation rates as a scaled gamma distribution to mimic the varying mutation baseline for different patients or disease subtypes. Resultantly, it modeled the mutation counts data using a two parameter negative binomial distribution, which improved the mutation counts fitting dramatically as compared to previous work (Fig. 2D).

Unlike previous efforts which use very limited covariates to estimate local mutation rate in very qualitative way, we explored the whole REMC and ENCODE data and searched for 381 features that best describe chromatin organization, expression profiling, replication status, and context effect in all possible tissues to jointly predict the local mutation rate at high precision. In terms of covariate correction, NIMBus demonstrates three obvious advantages: 1) it incorporates the most comprehensive covariates that provides the most accurate, at least to our knowledge, background mutation rate

estimation; 2) it provides an integrative framework that can be extended to any number of covariates and successfully avoids the high dimensionality problem as in other methods \{cite mutsigCV}. This is extremely important since the amount of available functional characteristic data is growing rapidly as the time and money cost of sequencing technologies drops; 3) it automatically utilizes the genomic regions with highest credibility for training purposes so potential users are not bothered to perform carefully calibrated training data selection and complex covariate matching processes.

In addition, we also put a lot of effort on NIMBus to explore the most extensive noncoding annotations. Noncoding regions represent more than 98% of the whole human genome, and are less investigated mainly due to limited knowledge to understand its biological functions. NIMBus collects the up to date full catalog of noncoding annotation of all possible tissue from the ENCODE project and our previous efforts from population genetics efforts in 1000 Genomes Project. All these included internal annotations of NIMBus can be either tested for somatic mutation burden or used to annotate the user specific input regions.

We applied NIMBus on 649 cancer genomes of 7 different types collected from public data and collaborators. The individual burden test P values for each cancer type have been deduced and then Fisher's method has been used to calculate the combined P values. As a result, a list of non-coding elements has been reported to have more than expected mutations (Table C in Fig. 5D). A list of already well-known regions, such as TP53, LMO, and TERT TSS, has also been reported in our analysis to be hypomutated, proving the effectiveness of NIMBus to identify functionally associated results.

It is worth mentioning that although we demonstrate the effectiveness of NIMBus mostly on somatic mutation analysis, it can be immediately extended to germline variant analysis as well. In summary, NIMBus is the first method that can integrate thousands of functional characteristic experimental data to analyze the mutation burdens in disease genomes. Such external data does not only help to better estimate the background mutation rate for successful false positive and negative control, but also provide the most extensive noncoding annotations for users to interpret their results. It may serve as a powerful computation tool to accurately predict driver events in human genetic disease and potentially identify biological targets for drug discovery.

Funding

Reference